

National Bureau of Standards

~~UNCLASSIFIED~~

U 8941

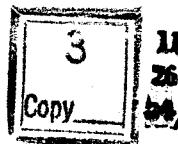
JUN 23 1945

HARVARD UNIVERSITY  
GRADUATE SCHOOL OF ENGINEERING

# OPERATOR METHODS IN THE THEORY OF COMPRESSIBLE FLUIDS

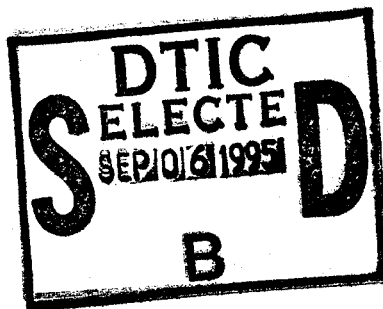
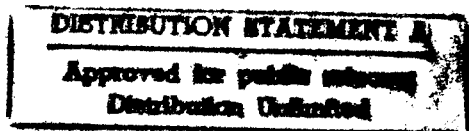
WORK PERFORMED UNDER CONTRACT NORD 8555 TASK F.

TECHNICAL REPORT NO. 12



*On Tables for the Determination of Transonic Flow Patterns*

BY STEFAN BERGMAN



CAMBRIDGE, MASS.

1949

19950831 145

DTIC QUALITY INSPECTED 5

U 8941

Offprinted from  
Reissner Anniversary Volume:  
Contributions to Applied Mechanics.  
J. W. Edwards, Ann Arbor, Michigan, 1949

## ON TABLES FOR THE DETERMINATION OF TRANSONIC FLOW PATTERNS\*

by

S. Bergman  
Harvard University  
Cambridge, Massachusetts

### INTRODUCTION

The equations for the stream functions of a steady, two-dimensional flow of a compressible fluid, which are non-linear when considered in the physical plane, become linear when transformed to the hodograph plane, see Ref. 11. In this latter plane, therefore, the principle of superposition can be applied. This, as well as the fact that the hodograph method is more suitable for the determination of pressure distribution on the boundary of the profile, suggests that the hodograph method be used in developing procedures for the computation of steady, two-dimensional flows.

The procedures for the computation of flow patterns by use of the hodograph method, especially the transformation back to the physical plane, require a very considerable amount of numerical work even in the case of an incompressible fluid. Moreover, the problem of determining the complex potential around a profile prescribed in the physical plane leads to very complicated non-linear boundary conditions when the hodograph method is used. There are at present no methods available for solving this problem directly. This makes it desirable to prepare tables based on the principle of the hodograph method but yielding the image of the streamlines directly in the physical plane. Thus the mathematical simplicity of the hodograph method could be exploited, and at the same time the bulk of the numerical work inherent in its use could be avoided. In the present paper a method for constructing such tables will be described.

In order to illustrate the principle along which such tables may be prepared, the preparation of the tables for

\*Research paper done under Navy Contract NOrd 8555-Task F at Harvard University. The ideas expressed in this paper represent the personal view of the author and are not necessarily those of the Bureau of Ordnance.

an incompressible fluid will first be explained. By making use of a correspondence principle introduced in Refs. 1, 3, 7, and 8, between incompressible and compressible flow, this method will be extended to a compressible fluid. Then two alternative methods will be discussed for setting up the tables, and a sample will be presented, prepared according to one of these. A numerical example illustrating the use of the tables will then be given. Finally, the conditions under which a given hodograph corresponds to a physically possible flow pattern will be discussed.

The author wishes to thank Dr. Bernard Epstein for valuable suggestions and Mr. Maurice Neuman for help in the preparation of the present paper.

#### NOTATION

- a - local velocity of sound, dependent upon the speed of the fluid
- $a_0$  - velocity of sound at the stagnation point
- k - ratio of isobaric to isovolumic specific heat
- p - pressure
- $p_0$  - pressure at the stagnation point
- q - speed
- x,y- Cartesian coordinates in the physical plane
- M - Mach number ( $M = q/a$ )
- $\theta$  - angle subtended by the velocity vector with the x-axis
- $\rho$  - density
- $\rho_0$  - density at the stagnation point which will be taken equal to 1
- $\sigma$  - a constant in the pressure density relation ( $p = \sigma \rho^k$ )
- $\varphi$  - potential function
- $\psi$  - stream function

Whenever a function is expressed in terms of two sets of variables obtained from each other by point transformations, the same symbol will be retained for both functional forms. Thus  $\psi(x,y) = \psi(q,\theta)$  when  $x = x(q,\theta)$  and  $y = y(q,\theta)$ .

In the present paper flow patterns will be considered which are characterized by three different equations of state:

- (1)  $\tilde{p} = p_0 = \text{const} = 1$  for an incompressible flow,
- (2)  $\rho = (p/\sigma)^{1/k}$  for an exact compressible flow,
- (3) an approximate form of (2) for a simplified compressible flow. (See the second section.)

Quantities pertaining to incompressible flow will be denoted by letters capped with tildas, e.g.,  $\tilde{H}$ ,  $\tilde{\psi}$ ,  $\tilde{X}^{(v)}$ ; quantities pertaining to exact compressible flow will be denoted by plain letters (except for superscripts), e.g.,  $H$ ,  $\psi$ ,  $X^{(v)}$ ; those referring to simplified compressible flow by letters with asterisks, e.g.,  $\psi^*$ ,  $X^*(v)$  etc.

## ON TABLES FOR AN INCOMPRESSIBLE FLUID

A plane is introduced whose Cartesian coordinates are the variables

$$\tilde{\eta} = \int^q \tilde{\rho}_0(dq/q) = \log q \quad (1)$$

and  $\theta$  (see notation).

The complex potential for a large class of symmetric obstacles in these variables can be written in the form

$$g(\tilde{z}) = \sum_{v=0}^{\infty} \tilde{b}_v (\tilde{z} - \eta_0)^{v-1/2} \quad (2)$$

with  $\tilde{z} = \tilde{\eta} + i\theta$  and  $\eta_0$  the logarithm of the speed at infinity. In the case of symmetric obstacles the  $b_v$ 's are purely imaginary (see Ref. 10, § 4).

Remark: The representation (2) holds only in a circle with origin at  $\tilde{\eta} = \eta_0$  and radius, the distance from  $\tilde{\eta} = \eta_0$  to the nearest singularity. However, by employing suitable summation methods, e.g.,

$$g(\tilde{z}) = \lim_{s \rightarrow \infty} \sum [\tilde{b}_v / \Gamma(1 + s_v)] [\tilde{z} - \eta_0]^{v-1/2} \quad (2a)$$

a representation is obtained for  $g(\tilde{z})$  in the largest doubly covered star domain in which the function is regular. (For details, see Ref. 12.) With the  $b_v$ 's purely imaginary, the stream function  $\tilde{\psi}$  can be written

$$\tilde{\psi} = \text{Im}[g(\tilde{z})] = \sum_{v=0}^{\infty} i \tilde{b}_v \tilde{\psi}^{(v)}(\tilde{\eta}, \theta; \eta_0) \quad (3)$$

$$\tilde{\psi}^{(v)}(\tilde{\eta}, \theta; \eta_0) = \text{Re}[\tilde{z} - \eta_0]^{v-1/2}$$

The streamlines of the flow patterns corresponding to  $g(\tilde{z})$  in the physical plane are given by

$$x = \sum_{v=0}^{\infty} 1b_v \tilde{X}^{(v)}(\tilde{\eta}, \theta; \eta_0), \quad y = \sum_{v=0}^{\infty} 1b_v \tilde{Y}^{(v)}(\tilde{\eta}, \theta; \eta_0) \quad (4)$$

where

$$\begin{aligned} \tilde{X}^{(v)}(\tilde{\eta}, \theta; \eta_0) = & \int (1/\tilde{\rho}_0 e^{\eta_0}) \{ [-\cos \theta \tilde{\psi}_{\theta}^{(v)} - \sin \theta \tilde{\psi}_{\tilde{\eta}}^{(v)}] d\eta \\ & + [\cos \theta \tilde{\psi}_{\tilde{\eta}}^{(v)} - \sin \theta \tilde{\psi}_{\theta}^{(v)}] d\theta \} \end{aligned} \quad (5a)$$

$$\begin{aligned} \tilde{Y}^{(v)}(\tilde{\eta}, \theta; \eta_0) = & \int (1/\tilde{\rho}_0 e^{\eta_0}) \{ [-\sin \theta \tilde{\psi}_{\theta}^{(v)} + \cos \theta \tilde{\psi}_{\tilde{\eta}}^{(v)}] d\eta \\ & + [\sin \theta \tilde{\psi}_{\tilde{\eta}}^{(v)} + \cos \theta \tilde{\psi}_{\theta}^{(v)}] d\theta \} \end{aligned} \quad (5b)$$

$b_v$ 's depend on the boundary curve of the profile. In employing the hodograph method in the incompressible fluid case, it is convenient to prepare a set of tables for

$$\tilde{\psi}^{(v)}(\tilde{\eta}, \theta; \eta_0), \quad \tilde{X}^{(v)}(\tilde{\eta}, \theta; \eta_0), \quad \tilde{Y}^{(v)}(\tilde{\eta}, \theta; \eta_0) \quad (6)$$

for a number of values of the parameter  $\eta_0$ . For, by using a set of  $b_v$ 's appropriate to the obstacle,  $\tilde{\psi}(\tilde{\eta}, \theta; \eta_0)$  could immediately be determined by making use of Eqs. (3) and (6). To find the image of a streamline

$$\tilde{\psi}(\tilde{\eta}, \theta; \eta_0) = s = \text{const} \quad (7)$$

in the physical plane, a sufficiently dense set of points  $(\tilde{\eta}_s, \theta_s) = 1, 2, \dots$ , is first found, corresponding to the streamline  $\tilde{\psi}(\tilde{\eta}, \theta; \eta_0) = s$ . From the tables values are read for

$$\tilde{X}^{(v)} = \tilde{X}^{(v)}(\tilde{\eta}_s, \theta_s; \eta_0), \quad Y^{(v)} = \tilde{Y}^{(v)}(\tilde{\eta}_s, \theta_s; \eta_0) \quad (8)$$

and by using Eq. (4) the image  $\tilde{\psi}(x, y) = s$  of  $\tilde{\psi}(\tilde{\eta}, \theta; \eta_0) = s$  is found in the physical plane.

The essence of this method is the separation of the quantities  $\tilde{X}^{(v)}$ ,  $\tilde{Y}^{(v)}$ ,  $\tilde{\psi}^{(v)}$  that are independent of the profile from the  $b_v$ 's which depend on it. For the former, a

set of tables can be prepared once and for all. The problem of determining the latter recurs with each profile. This is a relatively simple matter in the case of incompressible flow. New variables  $\tilde{\eta}$ ,  $\theta$  are introduced into the complex potential  $g(\tilde{z})$  and an expansion is made about  $\eta_0$ . The coefficients of the expansion are the desired  $\{b_v\}$ . In the compressible case the problem is much more involved, but in most cases of interest the  $b_v$ 's found for the incompressible case may be used in the compressible case as a first approximation to the exact  $b_v$ 's. Methods are known for improving on this approximation but this matter will not be discussed in the present paper.

#### EXTENSION OF THE METHODS USED IN THE CASE OF AN INCOMPRESSIBLE FLUID TO THE CASE OF A COMPRESSIBLE FLUID

The complex potential for the incompressible fluid flow considered in the  $\tilde{\eta}, \theta$  plane has (in general) singularities, such as branch points, poles, etc. The procedures developed for the treatment of this case make use of various properties of analytic functions defined on a Riemann surface. The recently developed theory of the integral operators permits the extension of these procedures to theory functions satisfying general partial differential equations, especially those satisfying the compressibility equation. (For details see Refs. 3, 4, 5, 7, 8.) In particular, a correspondence principle can be set up between the flow pattern of an incompressible fluid around a profile  $\tilde{C}$ , and that of a compressible fluid around a profile  $C$ , approximating  $\tilde{C}$ . It is easiest to display this correspondence principle if the equations for the compressible fluid case are transformed to the "quasi logarithmic" plane defined by the Cartesian coordinates  $(\eta, \theta)$

$$\eta(q) = \eta(q) = \int^q \rho(q) [dq/q] \quad (9)$$

with the constant of integration so chosen that  $\eta(a) = 0^{**}$ .

\*For the construction of flow patterns of an incompressible fluid around a given profile by the use of the hodograph method, see Ref. 14.

\*\*It is noted that in considering purely subsonic flows in previous papers the variable

$$\lambda = \int q^{-1} (1 - M^2) dq, \theta$$

was used and for purely supersonic flows the variable  $\lambda = i\lambda, \theta$ . In studying transonic flow patterns it is found to be more convenient to use the variables  $\eta, \theta$ .

Thus  $\eta < 0$  and  $\eta > 0$  for the sub- and supersonic ranges, respectively. In the incompressible case

$$\eta(q) = \tilde{\eta}(q) = \int^q \tilde{\rho}(dq/q) = \int^q (dq/q) \quad (9a)$$

where the constant of integration is now so chosen that  $\tilde{\eta}(q) = \log q$ . The transition from  $(\tilde{\eta}, \theta)$  to  $(\eta, \theta)$  means only a distortion in the  $\eta$  direction. In this coordinate system the compressibility equation becomes

$$L(\psi) = \partial^2 \psi / \partial \eta^2 + \ell(\eta) \partial^2 \psi / \partial \theta^2 = 0 \quad (10)$$

where

$$\ell(\eta) = [1 - M^2(\eta)] / \rho^2(\eta)$$

$M$  is the local Mach number,  $M = q/a(q)$ . (See Ref. 3, Par. 7.) For the incompressible case,  $M = 0$ ,  $\tilde{\rho} = \rho_0 = 1$  and Eq. (10) reduces to

$$\tilde{L}(\psi) = \partial^2 \tilde{\psi} / \partial \tilde{\eta}^2 + \partial^2 \tilde{\psi} / \partial \theta^2 = 0 \quad (10a)$$

From the expression for  $\ell(\eta)$  it is seen that the equation is elliptic in the subsonic and hyperbolic in the supersonic case.

By assuming an adiabatic pressure density relation  $p = \sigma \rho^k$  and employing the Bernoulli equation, the following explicit expression for  $a(q)$  and  $\rho(q)$  is found:

$$\left. \begin{aligned} \rho(q) &= \rho_0 \{ 1 - [(k-1)/2] (q/a)^2 \}^{1/(k-1)} \\ a^2(q) &= a_0^2(q) - [(k-1)/2] q^2 \end{aligned} \right\} \quad (11)$$

(See Ref. 1, p. 8-13.) Use of these formulas yields after a lengthy computation the following expression for  $\ell(\eta)$  (see Ref. 9, appendix).

$$\begin{aligned} \ell(\eta) &= 2[2/(k+1)]^{(2-k)/(k+1)} \{ -(2\eta) - \\ &\quad - [(3k+5)/(2k+2)] [2/(k+1)]^{-k/(k-1)} (-2\eta)^2 + \dots \} \quad (12) \end{aligned}$$

Eq. (10) is now simplified by retaining only the linear term in  $\eta$  of Eq. (12), i.e.,

$$\ell(\eta) = \ell^*(\eta) = C\eta, \quad C = -2[2/(k+1)]^{(2-k)/(k-1)} \quad (12a)$$

and writing

$$L^*(\psi) = \partial^2 \psi / \partial \eta^2 + C \eta \partial^2 \psi / \partial \theta^2 = 0^{++} \quad (10^*)$$

Remark: Tricomi (see Ref. 15) was the first to study Eq. (10\*) extensively. Different authors subsequently considered it in connection with the theory of compressible fluids. However, the present treatment is different from the treatments given previously. The "correspondence principle" is introduced and solutions of this equation defined on a Riemann surface and possessing singularities are considered. Eq. (10\*) will henceforth be referred to as the "simplified compressibility equation."

The application of the operator method to the solution of Eq. (10\*) will now be described. Every analytic function  $g$  of one complex variable  $z = \eta + i\theta$  can be written in the form

$$g(z) = m[f(z)] = \int_{-1}^{+1} \{ f[z(1-t^2)/2] / (1-t^2)^{1/2} \} dt \quad (11a)$$

with

$$f(z) = n[g(z)] = (2/\pi) \{ g(0) + z \int_{-1}^{+1} g'[2z(1-t^2)] dt \} \quad (11b)$$

where  $g'(\xi) = dg(\xi)/d\xi$ . It has been shown in Ref. 9 that for every equation of type (10\*) it is possible to define an operator  $p^*$  acting on  $g(z)$  such that

$$u^*(z) = p^*[g(z)] = p^* \{ m[f(z)] \} = P^*[f(z)] \quad (13)$$

is a complex solution of Eq. (10\*). The following are the explicit expressions for  $P^*[f(z)]$  and  $p^*[g(z)]$ :

$$P^*[f(z)] = \int_{-1}^{+1} E^*(\eta, \theta; \eta_0) f[(z/2)(1-t^2)] [(dt/\sqrt{1-t^2})] \quad (14)$$

$$p^*[g(z)] = S_0(-\eta)^{-1/4} \{ g(z) +$$

$$+ \sum (1/2^{2n}) [\Gamma(2n+1)/\Gamma(n+1)] p^n(z) g^{(n)}(z) \} \quad (15)$$

<sup>++</sup>This simplification is equivalent to replacing the exact pressure density relation by an approximate one. It is possible to show that the approximation to the exact equation of state is quite good in a certain range, in particular around the transonic line.



$E^*(\eta, \theta; \eta_0)$  may be taken as

$$E^*(\eta, \theta; \eta_0) = S_0(-\eta)^{-1/4} \mathcal{H}\{1/6, 5/6, 1/2, t^2[c(-\eta)^{3/2} + i\theta - \eta_0]/2c(-\eta)^{3/2}\} \quad (16)$$

where  $\mathcal{H}(\alpha, \beta, \gamma, X)$  is the hypergeometric function,  $S_0$  and  $c$  are numerical constants

$$\left. \begin{aligned} S_0 &= 2^{(2k+1)/(ek-e)} 2^{-1/e} (k+1)^{(2-k)/(ek-e)} \\ c &= (2^{3/2}/3) [(k-1)/2]^{(3k-e)/(ek-e)} \end{aligned} \right\} \quad (17)$$

The polynomials  $\mathbb{P}^{(n)}(z)$  are defined by the recursion formula and initial conditions:

$$\left. \begin{aligned} \mathbb{P}_z^{(1)} + 2F^* &= 0 \\ (2n+1)\mathbb{P}_z^{(n+1)}(z) + 2\mathbb{P}_{z\bar{z}}^{(n)} + 2F^*\mathbb{P}^n(z) &= 0 \\ \mathbb{P}^{(n)}(0) &= 0 \end{aligned} \right\} \quad (18)$$

with  $F^* = (5/36)(1/4c^2)(-\eta)^{-3}$

The functions  $g^{[n]}(z)$  may be written as

$$g^{[n]}[z] = \int_0^z \int_0^{z_1} \dots \int_0^{z_{n-1}} g(z_n) dz = [(-1)^n/(n-1)!] \int_{t=0}^{t=z} (z-t)^{n-1} g(t) dt \quad (19)$$

The method of integral operators permits setting up a correspondence principle between the flow patterns of an incompressible and a compressible fluid. Both fluids are considered in the quasi logarithmic plane (which in the case of an incompressible fluid reduces to the logarithmic plane). The correspondence principle consists in associating with the flow pattern  $\tilde{\psi} = \text{Im}[g]$  of an incompressible fluid a flow pattern  $\psi = \text{Im}[p^*(g)]$  of a compressible fluid. By introducing expansion (2) for  $g(\tilde{z})$  expressions are obtained for a compressible fluid that are the analogues of Eqs. (3), (4), and (5) for an incompressible fluid. Thus

$$p^*[g(z)] = \sum b_\nu p^*[(z - \eta_0)^{\nu-1/2}] \quad (20)$$

where

$$p^*[(z - \eta_0)^{\nu-1/2}] = B^{(\nu)}[p^*(z), \overline{p^*(z)}; \eta_0][p^*(z) - \eta_0]^{\nu-1/2} \quad (21)$$

and

$$p^*(z) = p^*[\eta + i\theta] = -c(-\eta)^{3/2} + i\theta = \zeta \quad (22)$$

$$\begin{aligned} B^{(v)}[p^*(z), \overline{p^*(z)}; \eta_0] &= B^{(v)}[\zeta, \bar{\zeta}; \eta_0] \\ &= S_0(-\eta)^{-1/4} \mathcal{H}[1/6, 5/6, v+1/2, (\zeta - \eta_0)/(-2c)(-\eta)^{3/2}] \quad (23) \end{aligned}$$

It is seen then that in the case of the stream function the transition from the incompressible to the compressible case is made by multiplying each term of its power series expansion by a "compressibility factor"  $B^{(v)}(\zeta, \bar{\zeta}; \eta_0)$  and by replacing the variable  $z = \eta + i\theta$  by the variable  $\zeta = -c(-\eta)^{3/2} + i\theta$ . This latter change implies a distortion in the  $\eta$  direction mentioned above.

Corresponding to expression (3) of the incompressible case, the stream function for a symmetric profile can be written in the form

$$\psi(\eta, \theta; \eta_0) = \sum 1 b_v \psi^{(v)}(\eta, \theta; \eta_0) \quad (24)$$

where

$$\psi^{(v)} = \text{Re}[B^{(v)}(\zeta, \bar{\zeta}; \eta_0)(\zeta - \eta_0)^{v-1/2}] \quad (25)$$

The implicit representation of the streamline  $\psi(\eta, \theta; \eta_0) = s$  in the physical plane is given by

$$x = \sum 1 b_v X^{(v)}(\eta, \theta; \eta_0), \quad y = \sum 1 b_v Y^{(v)}(\eta, \theta; \eta_0) \quad (26)$$

with

$$\begin{aligned} X^{(v)} &= \int (1/\rho) (1/e^{\int \sqrt{-\ell^*(\eta)} d\eta}) \{ [-(1-M^2)^{1/2} \sqrt{-\ell^*(\eta)} \psi_\theta^{(v)} \cos \theta - \psi_\eta^{(v)} \sin \theta] d\eta \\ &\quad + [(1-M^2)^{1/2} (\sqrt{-\ell^*(\eta)})^{-1} \psi_\eta^{(v)} \cos \theta - \psi_\theta^{(v)} \sin \theta] d\theta \} \quad (27a) \end{aligned}$$

$$\begin{aligned} Y^{(v)} &= \int (1/\rho) (1/e^{\int \sqrt{-\ell^*(\eta)} d\eta}) \{ [-(1-M^2)^{1/2} \sqrt{-\ell^*(\eta)} \psi_\theta^{(v)} \sin \theta - \psi_\eta^{(v)} \cos \theta] d\eta \\ &\quad + [(1-M^2)^{1/2} (\sqrt{-\ell^*(\eta)})^{-1} \psi_\eta^{(v)} \sin \theta + \psi_\theta^{(v)} \cos \theta] d\theta \} \quad (27b) \end{aligned}$$

In order to evaluate the "compressibility factors"  $B(v)(\eta, \theta; \eta_0)$ , suitable power series representations must be found for the hypergeometric function appearing in Eq. (23). It is well known that for  $|x| < 1$ ,  $\mathcal{H}(\alpha, \beta, \gamma, x)$  may be represented by a hypergeometric series  $F(\alpha, \beta, \gamma, x)$  and for  $|x| > 0$  a combination of two hypergeometric series with arguments and parameters different from those appearing in the hypergeometric function must be used (see Ref. 16, § IV). In the case of the hypergeometric function appearing in Eq. (23), the boundary separating the domains of convergence,

$$|[-c(-\eta)^{3/2} - \eta_0 + i\theta] / [-2c(-\eta)^{3/2}]| = 1$$

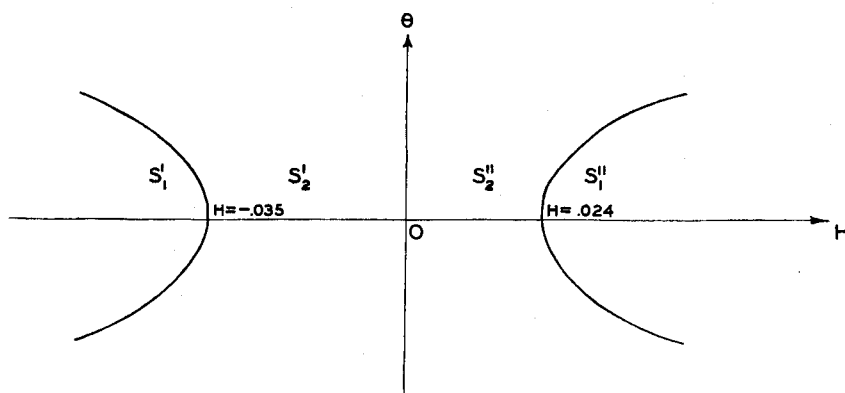


Fig. 1. Domains of Validity of the Power Series Representations (28a) and (28b) for the Hypergeometric Function

$$\mathcal{H}\left(\frac{1}{6}, \frac{5}{6}, v + \frac{1}{2}, \frac{-c(-\eta)^{3/2} - \eta_0 + i\theta}{-2c(-\eta)^{3/2}}\right)$$

$$(A) \quad 3c^2\eta^3 + \theta^2 + 2c(-\eta)^{3/2}\eta_0 + \eta_0^2 = 0 \quad \eta < 0$$

$$(B) \quad 3c^2\eta^3 - \theta^2 - 2c(-\eta)^{3/2}\theta - \eta_0^2 = 0 \quad \eta > 0$$

In  $S_1 = S'_1 + S''_1$  and in  $S_2 = S'_2 + S''_2$ , the representations

$$\mathcal{H}\left(\frac{1}{6}, \frac{5}{6}, +\frac{1}{2}, \frac{-c(-\eta)^{3/2} - \eta_0 + i\theta}{-2c(-\eta)^{3/2}}\right) = F\left(\frac{1}{6}, \frac{5}{6}, +\frac{1}{2}, \frac{-c(-\eta)^{3/2} - \eta_0 + i\theta}{-2c(-\eta)^{3/2}}\right) \quad (28a)$$

and

$$\begin{aligned}
 & \left( \frac{1}{6}, \frac{5}{6}, + \frac{1}{2}, \frac{-c(-\eta)^{3/2} - \eta_0 + 10}{-2c(-\eta)^{3/2}} \right) = \\
 & A_v \left( \frac{-2c(-\eta)^{3/2}}{-2c(-\eta)^{3/2} - \eta_0 + 10} \right)^{1/6} F \left( \frac{1}{6}, \frac{2}{3} - v, \frac{1}{3}, \frac{-2c(-\eta)^{3/2}}{-c(-\eta)^{3/2} - \eta_0 + 10} \right) + \\
 & B_v \left( \frac{-2c(-\eta)^{3/2}}{-2c(-\eta)^{3/2} - \eta_0 + 10} \right)^{5/6} F \left[ \frac{5}{6}, \frac{4}{3} - v, \frac{5}{3}, \frac{-2c(-\eta)^{3/2}}{-c(-\eta)^{3/2} - \eta_0 + 10} \right]
 \end{aligned}
 \tag{28b}$$

are used respectively. The  $A_v$ 's and  $B_v$ 's denote the quantities

$$A_v = \Gamma(-2/3)\Gamma(v + 1/2)/\Gamma(-1/3 - v)(5/6)$$

$$B_v = \Gamma(v + 1/2)\Gamma(2/3)/\Gamma(1/3 - v)\Gamma(1/6)$$

#### TABLES FOR A COMPRESSIBLE FLUID

It has been shown in the previous section how it is possible to extend the methods used in the case of an incompressible fluid to the case of a compressible one. The analogues of Eqs. (2), (3), (4), and (5) of the incompressible flow were obtained, namely Eqs. (20), (25), (26), and (27). These permit the setting up of tables for a compressible fluid of the type that was outlined in the first section for an incompressible fluid.

In this section two types of tables will be indicated. Type I depends upon a parameter  $\eta_0$  and has to be prepared for a number of values of  $\eta_0$ , say  $\eta_{0,v}$  ( $v = 1, \dots, n$ ). In this case one must resort to interpolation methods in order to obtain streamlines for intermediary values of  $\eta_0$ :  $\eta_{0,v} < \eta_0 < \eta_{0,v+1}$ . Tables of type II are independent of any parameter but their application requires more numerical work when used for a value of  $\eta_0$ , for which tables of type I are available.

Type I. In the present section a table of  $\psi^{(v)}(\eta, \theta; \eta_0)$  for a specific value of  $\eta_0$ ,  $\eta_0 = -.02$  will be given. A table is also included for

$$\varphi^{(v)}(\eta, \theta; -.02) = \text{Im}\{p^*[(z - .02)^{v-1/2}]\}$$

in view of possible later applications, and a conversion table from the variable  $\eta$  to the local Mach number  $M$ . An illustration of the use of these tables will be given in the next section.

TABLE I. VALUES OF THE FUNCTIONS  $\varphi^{(v)}(\eta, \theta)$ 

$\eta$	$\theta$	$v = 0$	$v = 1$	$v = 2$	$v = 3$	$v = 4$	$v = 5$
-.050	0.5	1.876	.015	-.869	-.043	.272	.025
	1.0	1.003	.012	-2.049	-.103	2.457	.209
	1.5	.802	.008	-2.983	-.161	8.419	.757
-.045	0.5	1.859	.015	-.854	-.043	.265	.024
	1.0	1.010	.010	-2.026	-.101	2.404	.214
	1.5	.798	.008	-2.951	-.164	8.577	.772
-.040	0.5	1.842	.016	-.838	-.042	.258	.023
	1.0	1.017	.010	-2.002	-.100	2.407	.217
	1.5	.794	.008	-2.920	-.165	8.696	.784
-.035	0.5	1.825	.016	-.824	-.041	.252	.023
	1.0	1.024	.010	-1.979	-.099	2.362	.213
	1.5	.790	.008	-2.888	-.167	8.832	.797
-.030	0.5	1.809	.016	-.809	-.040	.245	.022
	1.0	1.030	.010	-1.954	-.098	2.315	.208
	1.5	.785	.008	-2.857	-.168	8.929	.808
-.025	0.5	1.790	.016	-.793	-.040	.237	.021
	1.0	1.037	.010	-1.929	-.096	2.267	.204
	1.5	.781	.008	-2.825	-.170	9.115	.821
-.020	0.5	1.771	.016	-.778	-.039	.230	.021
	1.0	1.044	.010	-1.905	-.095	2.221	.200
	1.5	.777	.008	-2.794	-.171	9.252	.838
-0.015	0	9.669	0.157	0.002	—*	—	—
	0.5	1.754	0.017	-0.763	-0.038	0.223	0.020
	1.0	1.051	0.011	-1.88	-0.094	2.173	0.196
	1.5	0.805	0.007	-3.012	-0.156	8.274	0.734
-0.010	0	8.667	0.179	0.003	—	—	—
	0.5	1.737	0.017	-0.748	-0.037	0.215	0.019
	1.0	1.058	0.011	-1.857	-0.092	2.126	0.192
	1.5	0.810	0.007	-3.045	-0.157	8.139	0.721
-0.005	0	7.927	0.198	0.004	—	—	—
	0.5	1.715	0.017	-0.732	-0.037	0.208	0.019
	1.0	1.063	0.011	-1.830	-0.092	2.076	0.187
	1.5	0.813	0.008	-3.071	-0.155	7.985	0.715
0.005	0	13.222	0.472	0.012	—	—	—
	0.5	0.897	1.125	0.318	-0.359	0.072	0.102
	1.0	0.551	1.406	-0.841	-1.761	0.872	1.963
	1.5	0.416	1.604	-1.492	-4.454	3.350	11.146
0.010	0	11.839	0.516	0.013	—	—	—
	0.5	0.906	1.138	-0.310	-0.369	0.068	0.106
	1.0	0.555	1.417	-0.837	-1.785	0.847	2.014
	1.5	0.408	1.615	-1.474	-4.522	3.479	11.384

\* The dash indicates that the value is smaller than .0005

TABLE I. VALUES OF THE FUNCTIONS  $\varphi^{(v)}(\eta, \theta)$  (Cont.)

$\eta$	$\theta$	$v = 0$	$v = 1$	$v = 2$	$v = 3$	$v = 4$	$v = 5$
0.015	0	10.357	0.556	0.014	—*	—	—
	0.5	0.914	1.149	-0.302	-0.379	0.064	0.110
	1.0	0.557	1.423	-0.824	-1.811	0.819	2.058
	1.5	0.422	1.622	-1.458	-4.583	3.406	11.600
0.020	0	10.296	0.599	0.017	—	—	—
	0.5	0.922	1.161	-0.294	-0.388	0.059	0.113
	1.0	0.561	1.434	-0.813	-1.844	0.794	2.108
	1.5	0.423	1.63	-1.435	-4.644	3.333	11.818
.025	0.5	.931	1.173	-.286	-.398	.055	.117
	1.0	.565	1.445	-0.802	-1.876	.769	2.159
	1.5	.426	1.639	-1.426	-4.704	3.260	12.032
	0.5	.944	1.185	-.279	-.407	.051	.121
.030	1.0	.569	1.454	-.790	-1.908	.746	2.208
	1.5	.428	1.650	-1.411	-4.766	3.187	12.255
	0.5	.947	1.197	-.270	-.417	.046	.125
	1.0	.572	1.464	-.777	-1.939	.720	2.258
.035	1.5	.430	1.656	-1.395	-4.827	3.113	12.474
	0.5	.955	1.209	-.263	-.427	.043	.129
	1.0	.575	1.473	-.765	-1.969	.695	2.308
	1.5	.432	1.664	-1.379	-4.896	3.041	12.693
.040	0.5	.964	1.220	-.255	-.437	.038	.133
	1.0	.578	1.482	-.753	-2.000	.670	2.359
	1.5	.434	1.66	-1.363	-4.933	2.968	12.918
	0.5	.973	1.231	-.247	-.446	.035	.137
.050	1.0	.582	1.491	-.741	-2.031	.645	2.410
	1.5	.433	1.671	-1.347	-5.009	2.896	13.142

\*The dash indicates that the value is smaller than .0005

TABLE II. THE VALUES OF FUNCTIONS  $\psi^{(\nu)}(\eta, \theta)$ 

$\eta$	$\theta$	$\nu = 0$	$\nu = 1$	$\nu = 2$	$\nu = 3$	$\nu = 4$	$\nu = 5$
-0.050	0.5	.017	.668	.020	-.234	-.017	.069
	1.0	.012	1.688	.051	-2.299	-.162	2.686
	1.5	.007	1.935	.053	-5.697	-.281	14.761
-.045	0.5	.017	.644	.019	-.223	-.016	.065
	1.0	.013	1.706	.051	-2.260	-.153	2.619
	1.5	.007	1.926	.053	-5.628	-.292	14.517
-.040	0.5	.017	.619	.019	-.212	-.015	.062
	1.0	.013	1.694	.051	-2.224	-.156	2.564
	1.5	.007	1.916	.053	-5.558	-.350	14.268
-.035	0.5	.017	.593	.018	-.200	-.014	.058
	1.0	.013	1.684	.051	-2.190	-.154	2.510
	1.5	.007	1.907	.054	-5.488	-.385	14.019
-.030	0.5	.016	.565	.017	-.188	-.013	.054
	1.0	.013	1.673	.050	-2.154	-.151	2.453
	1.5	.007	1.901	.054	-5.419	-.379	13.769
-.025	0.5	.016	.535	.016	-.180	-.012	.050
	1.0	.013	1.662	.050	-2.117	-.148	2.395
	1.5	.007	1.888	.055	-5.346	-.375	13.513
-.020	0.5	.016	.500	.015	-.161	-.011	.046
	1.0	.014	1.649	.049	-2.081	-.145	2.285
	1.5	.007	1.879	.054	-5.277	-.369	13.263
-0.015	0	9.517	0.478	0.013	—*	—	—
	0.5	0.042	1.317	0.039	-0.417	-0.029	0.117
	1.0	0.013	1.641	0.047	-2.045	-0.143	2.281
	1.5	0.007	1.840	0.052	-5.203	-0.357	13.000
-0.010	0	10.416	0.446	0.011	—	—	—
	1.5	0.043	1.303	0.039	-0.406	-0.028	0.112
	1.0	0.013	1.629	0.049	-2.009	-0.141	2.222
	1.5	0.007	1.860	0.054	-5.134	-0.358	12.732
-0.005	0	11.478	0.411	0.009	—	—	—
	0.5	0.044	1.289	0.038	-0.394	-0.027	0.107
	1.0	0.014	1.616	0.048	-1.970	-0.138	2.161
	1.5	0.007	1.847	0.054	-5.050	-0.352	12.470
0.005	0	-0.002	0.002	—	—	—	—
	0.5	-1.432	0.616	0.652	-0.154	-0.193	0.0332
	1.0	-0.914	0.788	1.601	-0.868	-1.866	0.862
	1.5	-0.700	0.908	2.739	-2.323	-7.086	5.362
0.010	0	-0.001	—	—	—	—	—
	0.5	-1.418	0.611	0.667	-0.148	-0.199	0.031
	1.0	-0.909	0.784	1.631	-0.852	-1.908	0.830
	1.5	-0.687	0.904	2.773	-2.288	-7.218	5.227

\* The dash indicates that the value is smaller than .005.

TABLE II. THE VALUES OF FUNCTIONS  $\psi^{(v)}(\eta, \theta)$  (Cont.)

$\eta$	$\theta$	$v = 0$	$v = 1$	$v = 2$	$v = 3$	$v = 4$	$v = 5$
0.015	0	-0.002	—*	—	—	—	—
	0.5	-1.403	0.604	0.679	-0.142	-0.205	0.027
	1.0	-0.901	0.777	1.649	-0.831	-1.943	0.795
	1.5	-0.696	0.900	2.800	-2.252	-7.377	5.091
0.020	0	-0.283	0.007	-0.001	—	—	—
	0.5	-1.386	0.597	0.692	-0.135	-0.211	0.024
	1.0	-0.895	0.773	1.672	-0.814	-1.983	0.765
	1.5	-0.691	0.895	2.8220	-2.215	-7.456	4.952
.025	0.5	-1.371	.591	.705	-.129	-.218	.022
	1.0	-.890	.769	1.695	-.796	-2.023	.733
	1.5	-.687	.891	2.854	-2.179	-7.574	4.815
.030	0.5	-1.350	.585	.719	-.123	-.224	.019
	1.0	-.884	.768	1.716	-.777	-2.067	.702
	1.5	-.684	.889	2.882	-2.143	-7.694	4.678
.035	0.5	-1.340	.578	.731	-.117	-.230	.017
	1.0	-.877	.758	1.736	-.758	-2.108	.670
	1.5	-.680	.882	2.909	-2.106	-7.814	4.540
.040	0.5	-1.325	.571	.744	-.111	-.237	.014
	1.0	-.871	.753	1.757	-.739	-2.149	.638
	1.5	-.676	.877	2.936	-2.067	-7.933	4.406
.045	0.5	-1.309	.565	.757	-.105	-.243	.011
	1.0	-.864	.748	1.778	-.721	-2.190	.606
	1.5	-.673	.877	2.963	-2.018	-8.054	4.271
.050	0.5	-1.293	.558	.771	.099	-.250	.009
	1.0	-.858	.743	1.798	-.702	-2.231	.575
	1.5	-.678	.871	2.990	-1.997	-8.175	4.135

\* The dash indicates that the value is smaller than .005.



TABLE III

Conversion of M to  $\eta$ 

M	$\eta$	M	$\eta$
.60	-.1977	.96	-.0165
.62	-.1857	.98	-.0083
.64	-.1750	1.00	0
.66	-.1616	1.01	.0044
.68	-.1541	1.02	.0079
.70	-.1407	1.03	.0120
.72	-.1307	1.04	.0160
.74	-.1195	1.05	.0197
.76	-.1087	1.06	.0234
.78	-.0978	1.07	.0274
.80	-.0887	1.08	.0312
.82	-.0787	1.09	.0350
.84	-.0692	1.10	.0387
.86	-.0603	1.10	.0387
.88	-.0513		
.90	-.0421		
.92	-.0336		
.94	-.0245		

Type II. In preparing this type of table the values of  $\mathcal{H}(1/6, 5/6, \nu + 1/2, \alpha + i\beta)$  are computed once and for all, as well as its derivative with respect to the argument for a number of values of  $\alpha$  and  $\beta$  where

$$\alpha = 1/2 - \eta_0 / [-2c(-\eta)^{3/2}] \quad \beta = \theta / [-2c(-\eta)^{3/2}]$$

By the use of tables of fractional powers and trigonometric functions and the tables outlined above, the computation can now be made,

$$\psi^{(\nu)} = \text{Re}[S_0(-\eta)]^{1/4} [-c(-\eta)^{3/2} - \eta_0 + i\theta]^{-1/2} \mathcal{H}(1/6, 5/6, \nu + 1/2, \alpha + i\beta)$$

$$\text{and } \psi_{\theta}^{(\nu)}(\eta, \theta; \eta_0), \quad \psi_{\eta}^{(\nu)}(\eta, \theta; \eta_0).$$

The stream functions in the hodograph plane are obtained by forming  $\psi(\eta, \theta; \eta_0) = \sum i b_{\nu} \psi^{(\nu)}(\eta, \theta; \eta_0)$ . The integrals of Eqs. (27a) and (27b) are now evaluated by using the tables for the derivative of  $\mathcal{H}(1/6, 5/6, \nu + 1/2, \alpha + i\beta)$ .

The transition to the physical plane is carried out by numerical integration of Eqs. (27a) and (27b).

Note. Since the integrands of Eq. (17) are perfect differentials, the value of the integral is independent of the path and it may conveniently be taken along a streamline.

Tables of Type II will not be given in the present paper.

#### ILLUSTRATION OF THE USE OF THE TABLES

As in a previous paper<sup>10</sup> the complex potential of an incompressible fluid flow around an elliptic profile is chosen as the analytic function  $g(z)$ . As is well known, the complex potential of an incompressible flow around a circle is given in the physical plane ( $t$  plane) by the relation

$$w = \varphi + i\psi = q_0(t + R/t^2) \quad (29)$$

where  $q_0$  is the dimensionless speed at infinity. The function

$$\xi = (1/2)(t + 1/t) \quad (30)$$

maps the exterior of the circle onto the exterior of the ellipse and therefore the function  $g(\xi) = w[t(\xi)]$  will represent the complex potential of an incompressible flow around an ellipse in the physical plane. This potential when transformed to the hodograph plane will furnish, upon expansion about  $\eta_0$ , a set of  $\{b_v\}$  for the incompressible case, which, as a first approximation will also be used for the compressible flow. (See the first section.)

This transformation is carried out as follows: The conjugate to the velocity vector  $\bar{q}$  is given by

$$q = dw/d\xi = (dw/dt)/(d\xi/dt) = [(1/2)q_0(1 - R^2/t^2)]/[(1/2)q_0(1 - 1/t^2)] \quad (31)$$

or

$$t^2 = (q - q_0 R^2)/(q - q_0) \quad (32)$$

where  $q_0$  is the velocity at infinity.

Therefore,

$$w\{\xi[t(q)]\} = (1/2)q_0\{[(\bar{q} - q_0 R^2)/(\bar{q} - q_0)]^{1/2} + R^2[(\bar{q} - q_0)/(\bar{q} - q_0 R^2)]^{1/2}\} \quad (33)$$

Since the complex potential in the logarithmic plane is needed,  $z$  is set  $= \tilde{\eta} - i\theta$  with  $\tilde{\eta} = \int^q dq/q = \log q$  and  $\eta_0 = \log q_0$ . Thus is obtained

$$q(z) = (1/2)\text{Re}(e^{\eta_0}) \{ [(1 - R^{-2}e^{z-\eta_0})/(1 - e^{z-\eta_0})]^{1/2} + [(1 - e^{z-\eta_0})/(1 - R^{-2}e^{z-\eta_0})]^{1/2} \} \quad (34)$$

which can be developed in a power series of the form

$$g(z) = \sum_{v=0}^{\infty} b_v (z - \eta_0)^{v-1/2} \quad (34a)$$

As an example,  $q_0$  is taken equal to 0.98 (or  $\eta_0 = -0.02$ ) and  $R^2 = 1.2$ , which yields a thickness ratio for the elliptic profile of 11:1. With these numerical values for  $u$  and  $R$  the set of  $\{b_v\}$  listed in Table IV is obtained.

TABLE IV

The Series Coefficients of Function  $g$

$v$	0	1	2	3	4	5
$b$	.240101	-2.100861	-4.859411	-8.170151	-82.869231	-389.551

It is observed that the radius of convergence of this series is  $|\zeta - \eta_0| = \log R^2 = .18$  about the center  $\zeta = \eta_0$ . As was mentioned before, however, by employing suitable summation methods, the series may be used outside its domain of convergence (see the first section).

Using these values for  $\{b_v\}$  and the table of  $\{\psi(v)\}$  yields the expression

$$\psi = \sum v b_v \psi^{(v)}(\eta, \theta; -0.02)$$

which is equated to zero. If this is solved by a graphical method, a number of points are obtained on the streamline

$$\psi(\eta, \theta; -0.02) = 0 \quad (35)$$

(see Table V).

TABLE V

Points on Streamline  $\psi(\eta, \theta; -0.02) = 0$ 

$\eta$	.032	.029	.025	.014	0	-.014
$\theta$	0	.08	.124	.151	.170	.190

The next task is to obtain the image of this streamline in the physical plane. To do this the values of  $\{X^{(v)}\}$  and  $\{Y^{(v)}\}$   $v = 0, 1, \dots, 5$ , are found corresponding to the set  $(\eta, \theta)$ . (See Tables VI and VII.)

TABLE VI

Values of  $X^{(v)}$  ( $\eta, \theta; -0.02$ ) for Points on Streamline  $\psi(\eta, \theta; -0.02) = 0$ 

$\eta$	$\theta$	$X^{(0)}$	$X^{(1)}$	$X^{(2)}$	$X^{(3)}$	$X^{(4)}$	$X^{(5)}$
.032	0	.26080	.32965	.02475	.00034	.00001	0
.029	.08	-7.44056	-2.19674	2.10610	.09443	-.04773	-.00019
.025	.124	4.18929	.92197	.45728	.13936	-.00931	.00272
.014	.151	3.57784	3.41533	1.43748	.59867	-.15616	.00155
0	.170	.30167	-.04313	.02595	.00582	-.00119	-.00032
-.014	.190	8.00948	-1.78920	-1.86983	-.44607	.15081	.03738

TABLE VII

Values of  $Y^{(v)}$  ( $\eta, \theta; -0.02$ ) for Points on Streamline  $\psi(\eta, \theta; -0.02) = 0$ 

$\eta$	$\theta$	$Y^{(0)}$	$Y^{(1)}$	$Y^{(2)}$	$Y^{(3)}$	$Y^{(4)}$	$Y^{(5)}$
.032	0	0	0	0	0	0	0
.029	.08	.46713	-.17611	.16885	.00758	-.00383	-.00001
.025	.124	.52218	.11492	.05700	.01737	-.00119	.00034
.014	.151	.54465	.51988	.21895	.09112	-.02377	.00025
0	.170	.05173	-.00740	.00445	.00100	-.00020	-.00005
-.014	.190	1.02992	-.22806	-.23916	-.05751	.01908	.00481

By forming the expressions

$$x = \sum 1b_v X^{(v)}(\eta, \theta; -0.02)$$

$$y = \sum 1b_v Y^{(v)}(\eta, \theta; -0.02)$$

a set of points is obtained lying on the streamline  $\psi = 0$  in the physical plane (see Table VIII).

TABLE VIII

Points on the Streamline  $\psi(\eta, \theta; -0.02) = 0$  in the Physical Plane

$\eta$	.032	.029	.025	.014	0	-.014
$\theta$	0	.08	.124	.151	.170	.190
$M$	1.080	1.072	1.057	1.035	1	.969
$x$	-2.71	-4.68	-10.71	-21.68	-21.78	-25.23
$y$	4.364	4.204	3.454	1.594	1.574	1.084

Fig. 2 represents the streamline of the incompressible flow  $\tilde{\psi}(x, y) = 0$ , coinciding with the boundary curve of the

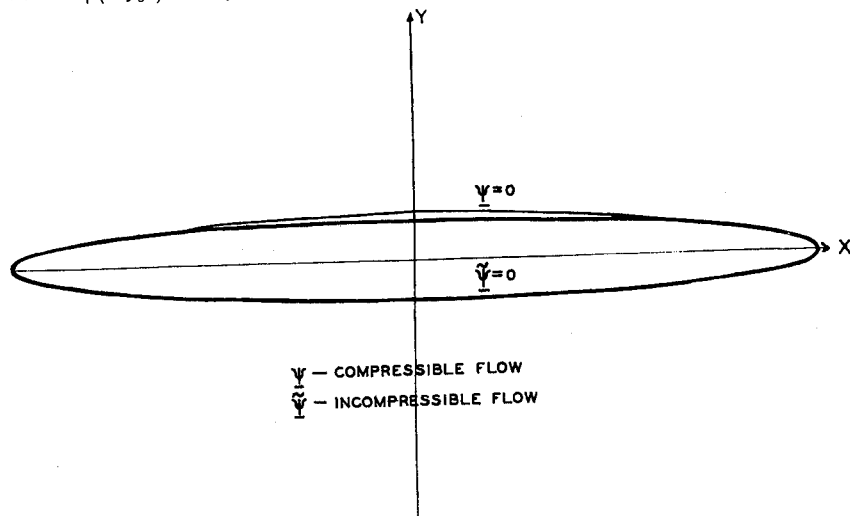


Fig. 2. Parts of the Streamlines  $\psi(x, y) = 0, \tilde{\psi}(x, y) = 0$  about Oval-shaped Obstacles  $C$  and  $\tilde{C}$  respectively.

obstacle together with the streamline  $\psi(x,y) = 0$  of the compressible flow. In setting up the diagram, the two streamlines were drawn in different scales in order to make the terminal points of the two ovals coincide. The neighborhood of the terminals of the ovals in the physical plane corresponds to the neighborhood of low Mach numbers in the hodograph plane. The streamline in these neighborhoods in the former plane is obtained by expanding  $X^{(v)}(\eta, \theta; \eta_0)$  and  $Y^{(v)}(\eta, \theta; \eta_0)$  in terms of the Mach number as a parameter of smallness:

$$X^{(v)}(\eta, \theta; \eta_0) = \bar{X}^{(v)}(\bar{\eta}, \theta; \eta_0) + M X_1^{(v)}(\bar{\eta}, \theta; \eta_0) + \dots$$

$$Y^{(v)}(\eta, \theta; \eta_0) = \bar{Y}^{(v)}(\bar{\eta}, \theta; \eta_0) + M Y_1^{(v)}(\bar{\eta}, \theta; \eta_0) + \dots$$

where  $X(\eta, \theta; \eta_0)$ ,  $Y(\eta, \theta; \eta_0)$  are defined by Eqs. (5a) and (5b). Only the part of the streamline located in the upper half of the physical plane has been plotted in the diagram. The part in the lower half is symmetric to it with respect to the x-axis.

#### CONDITIONS UNDER WHICH A GIVEN HODOGRAPH CORRESPONDS TO A PHYSICALLY POSSIBLE FLOW PATTERN

In the considerations of the previous sections the question was completely disregarded as to whether the flow pattern obtained by this method is of physical significance. Obviously, if the function  $\psi(x,y)$  is to yield a flow pattern around a closed profile in the physical plane, it is necessary that

(a) the streamline  $\psi(x,y) = 0$  (or a part of this streamline, in the present case the image of the lines ABA'B', see Fig. 3) yield a closed curve in the physical plane;

(b) that every point of the physical plane be covered at most once (that is, that the mapping unto the x,y-plane be schlicht\*).

The two conditions for the subsonic case will now be considered:

\*It is remarked, however, that if the whole image in the x,y-plane is not schlicht, the flow pattern obtained may nevertheless be of physical interest since in some instances it is required to determine flow patterns covering only part of the x,y-plane or only a part of the flow pattern obtained is used.

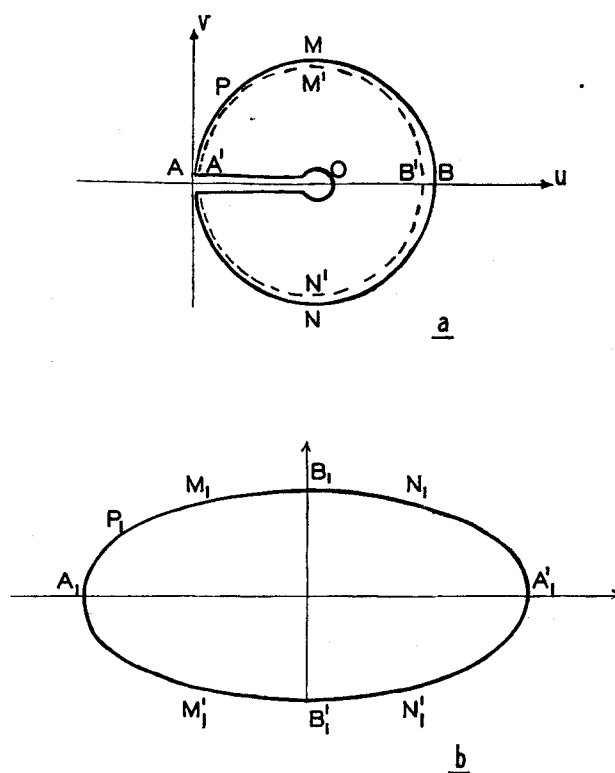


Fig. 3. The Streamline  $\psi = 0$  in the Hodograph and Physical Planes.

(a') The necessary and sufficient conditions that the boundary  $AB A'B'$  when mapped by Eq. (26) unto the physical plane yield a closed curve in the latter plane have been established in a previous paper for flow patterns that are not necessarily symmetric. (See Ref. 7.)

(b') The determinant of the mapping from the hodograph to the physical plane  $\partial(x,y)/\partial(u,v)$  is always positive. It is therefore sufficient and necessary, in order that the mapping be schlicht, that the boundary curve  $A_1B_1 A'_1B'_1$  be schlicht, and that the mapping satisfy certain regularity conditions at infinity, which will be stated presently.

In the case under consideration the schlichtness of the boundary curve  $A_1B_1 A'_1B'_1$  follows from the symmetry of the image in the hodograph plane and the fact that the hodograph

lies in the half plane  $u > 0$ . Indeed, if the point P moves along a line AMP, then the velocity component 'u' is always positive, that is, the x coordinate always increases. The segment BNA' cannot intersect itself or the arc ANB, since the coordinate still increases if the point P moves along this curve. From the symmetry properties it follows that this arc lies in the upper half, and that the image of A'N'B'A', in the lower half of the xy- plane. The whole boundary curve is then schlicht. The mapping must satisfy the following conditions at infinity: As a doubly covered circle about the point 0 the image of infinity of the hodograph plane shrinks to a point, its image in the inverted physical plane  $[x' + iy' = 1/(x + iy)]$  must be schlicht and also shrink to a point.

In generalizing these results to transonic flow patterns, one must be on guard against the following difficulties:

(a) The functional determinant  $\partial(u,v)/\partial(x,y)$  is not necessarily positive,

(b) The mixed character of the equation of flow may give rise to hyperbolic singularities which do not appear in the subsonic case.

The general character of mappings of this type has been extensively investigated by Morse and others (see Ref. 13). This problem will not be discussed in the present paper.

#### REFERENCES

1. Bergman, S., The Hodograph Method in the Theory of Compressible Fluids. Supplement to Fluid Dynamics by von Mises and Friedrichs, Brown University 1941-1942.
2. Bergman, S., Partial Differential Equations, Advanced Topics. Brown University 1941.
3. Bergman, S., On Two-Dimensional Flows of Compressible Fluids. Technical Note 972, National Advisory Committee for Aeronautics, 1945, pp. 1-8.
4. Bergman, S., Graphical and Analytic Methods for the Determination of a Flow of a Compressible Fluid around an Obstacle. Technical Note 973, National Advisory Committee for Aeronautics, 1945, pp. 1-29.
5. Bergman, S., Certain Classes of Analytic Functions of Two Real Variables and Their Properties. Trans. of American Mathematical Society, Vol. 57, 1945, pp. 299-331.
6. Bergman, S., Method for the Determination and Computation of Flow Patterns of a Compressible Fluid. Technical Note 1018, National Advisory Committee for Aeronautics, 1946. pp. 1-71.



7. Bergman, S., Two-Dimensional Subsonic Flows of a Compressible Fluid and Their Singularities. Trans. of American Mathematical Society, Vol. 62, 1947, pp. 452-498.
8. Bergman, S., Two-Dimensional Transonic Flow Patterns. American Journal of Mathematics, Vol. 70, 1948. For Appendix to this Paper See "Operator Methods in the Theory of Compressible Fluids," Report 10.
9. Bergman, S., Solutions of Linear Partial Differential Equations of Fourth Order. Duke Mathematics Journal, Vol. 11, No. 3, 1944, pp. 617-649.
10. Bergman, S. and Epstein, B., Determination of a Compressible Fluid Flow Past an Oval-Shaped Obstacle. Journal of Mathematics and Physics, Vol. 26, No. 4, 1948, pp. 195-222.
11. Chaplygin, S. A., On Gas Jets. Scientific Memoirs, Moscow Univ. Math. Phys. Sec. 21, 1902, pp. 1-121.
12. Lindelof, E., Calcul des Residues, Paris, 1905.
13. Morse, M., Topological Methods in the Theory of Functions of a Complex Variable. Princeton University Press, 1947.
14. Simonov, L. A., Calculation of an Aerofoil in a Flow and Plotting of an Aerofoil According to a Distribution of Velocities Over Its Surface. Applied Mathematics and Mechanics [Akad. Nauk. SSSR. Prikl. Mat Mech.] 11, 69-84, 1947. [Russian. English Summary]
15. Tricomi, F., Sulle equazioni lineari alle derivate parziali di 2° ordine di tipo misto. Memorie della R. Acc. Naz. d. Lincei, Vol. 14, 1923, pp. 133-247.
16. Whittaker, E. T., and Watson, G. N., A Course of Modern Analysis, New York, 1945.

Accession For	
NTIS GRA&I	<input checked="" type="checkbox"/>
DTIC TAB	<input type="checkbox"/>
Unannounced	<input type="checkbox"/>
Justification	
By	
Distribution/	
Availability Codes	
Dist	Avail and/or Special
A-1	20

## PREVIOUS PUBLICATIONS

1. Classes of solutions of linear partial differential equations in three variables. Stefan Bergman. Duke Mathematical Journal, Volume 13, 1946, pp. 419-458.
2. Models in the theory of several complex variables. Stefan Bergman. American Mathematical Monthly. Volume 53, 1946, pp. 495-501.
3. Punch-card machine methods applied to the solution of the torsion problem. Stefan Bergman. Quarterly of Applied Mathematics. Volume 5, 1947, pp. 69-81.
4. Determination of the coefficients of the integral operator by use of punch-card machines. S. Bergman and L. Greenstone. Journal of Mathematics and Physics, Volume 26, 1947, pp. 1-9. [Report 1-NOrd 8555 Task F.]
5. Two-dimensional subsonic flows of a compressible fluid and their singularities. Stefan Bergman. Transactions of the American Mathematical Society, Volume 61, 1947, pp. 452-498. [Report 2-NOrd 8555 Task F.]
6. Determination of the coefficients of the integral operator by interpolatory means. Rufus Isaacs. Journal of Mathematics and Physics, Volume 26, 1947, pp. 165-181. [Report 3-NOrd 8555-Task F.]
7. Functions satisfying certain partial differential equations of elliptic type and their representation. Stefan Bergman. Duke Mathematical Journal, Volume 14, 1947, pp. 349-366. [Report 4-NOrd 8555-Task F.]
8. A representation of Green's and Neumann's functions in the theory of partial differential equations of the second order. Stefan Bergman and M. Schiffer. Duke Mathematical Journal, Volume 14, 1947, pp. 609-638. [Report 5-NOrd 8555-Task F.]
9. On Green's and Neumann's functions in the theory of partial differential equations. S. Bergman and M. Schiffer. Bulletin of the American Mathematical Society, Volume 53, 1947, pp. 1141-1151. [Report 6-NOrd 8555-Task F.]
10. Determination of a compressible fluid flow past an oval-shaped obstacle. S. Bergman and B. Epstein. Journal of Mathematics and Physics, Volume 26, 1947, pp. 195-218. [Report 11-NOrd 8555-Task F.]
11. Some inequalities relating to conformal mapping upon canonical slit-domains. Bernard Epstein. Bulletin of the American Mathematical Society, Volume 53, 1947, pp. 813-819.
12. An application of orthonormal functions in the theory of conformal mapping. M. Schiffer. American Journal of Mathematics, Volume 70, 1948, pp. 147-156.
13. On Bergman's integration method in two-dimensional compressible fluid flow. R. von Mises and M. Schiffer. Advances of Mechanics, Volume 1, Academic Press, Inc., 1948. [Report 7-NOrd 8555-Task F.]
14. Kernel functions in the theory of partial differential equations of elliptic type. S. Bergman and M. Schiffer. Duke Mathematical Journal, Volume 15, 1948, pp. 535-566. [Report 1-N5ori 76-16.]
15. Identities in the theory of conformal mapping. P. R. Garabedian and M. Schiffer. Transactions of the American Mathematical Society, Volume 64, 1948. [Report 2-N5ori 76-16.]
16. An initial value problem for equations of mixed type. S. Bergman. Bulletin of the American Mathematical Society, Volume 55, 1949, pp. 165-174. [Report 9-NOrd 8555-Task F.]
17. Sur les fonctions orthogonales de plusieurs variables complexes avec les applications à la théorie des fonctions analytiques. Stefan Bergman. Mémorial des Sciences Mathématiques, Volume 106, 1947.
18. Functions of extended class in the theory of functions of several complex variables. Stefan Bergman. Transactions of the American Mathematical Society, Volume 63, 1948, pp. 523-547.

(Continued on next page)

(Continued from previous page)

19. Two-dimensional transonic flow patterns. Stefan Bergman. American Journal of Mathematics, Volume 70, 1948. [Report 10-NOrd 8555-Task F.]
20. The kernel function in canonical maps. Z. Nehari. Duke Mathematical Journal, Volume 16, 1949, pp. 165-178. [Report 3-N5ori 76-16.]
21. Reproducing and pseudo-reproducing kernels and their application to the partial differential equations of physics. N. Aronszajn. Studies in Partial Differential Equations. Harvard Graduate School of Engineering, Cambridge, Massachusetts, 1948.
22. On tables for the determination of transonic flow patterns. Stefan Bergman. Hans Reissner Anniversary Volume. Brooklyn Polytechnic Institute, 1949. [Report 12-NOrd 8555-Task F.]
23. The regularity domains of solutions of linear partial differential equations in terms of the series development of the solution. Benham Ingersoll. Duke Mathematical Journal, Volume 15, 1948. [Report 2-N5ori 76-16.]
24. Schwarz's lemma and the Szegő kernel function. Paul R. Garabedian. Transactions American Mathematical Society, Volume 64, 1949. [Report 7-N5ori 76-16.]
25. Operator methods in the theory of compressible fluids. Stefan Bergman. First Symposium in Applied Mathematics. The American Mathematical Society. [Report 8-NOrd 8555-Task F.]
26. Sur la fonction-noyau d'un domaine et ses applications dans la théorie des transformations pseudo-conformes. Stefan Bergman. Mémorial des Sciences Mathématiques, Volume 108, 1948.
27. Distortion of length in conformal mapping. P. R. Garabedian. Duke Math. Journal. [Report 4-N5ori 76-16.]
28. The algebraic character of a class of harmonic functions in three variables. P. Pepper. Bulletin of Am. Math. Soc., 1949. [Report 8-N5ori 76-16.]
29. On different types of orthogonalization. M. Schiffer. Duke Math. Journal. [Report 14-N5ori 76-16.]
30. Kernel functions and canonical mapping. S. Bergman and M. Schiffer. Duke Math. Journal. [Report 15-N5ori 76-16.]